Analysis of Natural Frequencies of Marine Turbine Blades

Pascal Stephan
pascal.stephan@tecnico.ulisboa.pt
Instituto Superior Técnico, Universidade de Lisboa, Portugal
September 2018

Tidal Energy has great potential for certain countries, which have projects underway for electricity generation capacity up to 400 MW with the help of Marine Current Turbines. Therefore, it is of crucial importance to be able to build reliable and durable turbines with little maintenance due to their difficult accessibility. Previous works performed by T. Clara (2014) and Young et. al (2010) focussed on vibrational mode shapes as well as natural frequencies of the blades. The problem was that disagreements in the results occurred between these scientific articles. A detailed investigation of different approaches of computing the natural frequencies in air and water for simple structures and the given turbine blade is presented in this work. All required computations have been performed in the commercial finite element software Abaqus and results have been compared to analytical formulations, where applicable. Numerical convergence studies have been carried out and the results for the different configurations have been compared with the results of Clara (2014) and Young et al (2010). It has been realized, that results lie within the same magnitude as the previously performed work of Clara (2014).

Coupled Fluid-Structure Interaction, Natural Frequency, Acoustic Elements, Marine Current Turbine

1. INTRODUCTION

Since the beginning of human mankind, energy production has always been a driving factor for development and living. Latest with the industrial revolution beginning of the 19th century and the invention of the steam engine large-scale energy production became one of the most important factors for industrial manufacturing.

It occurred that the exploitation of different available natural resources expanded and finally energy production based on carbon and oil overtook the natural resources becoming the worldwide leading position. As generally known, this development brought the negative effect of emission of harmful pollutants into the atmosphere and also resulted in a steep increase of the carbon dioxide concentration.

As a consequence more investigations with particular regards to water resources have been performed (Rossi, Righetti and Renzi 2016).

1.1 Renewable Energy

Policies of most industrialized countries have come to the conclusion that implementing Renewable Energy Sources into their energy markets is one key factor in reducing the production of greenhouse gas emissions (Ramos 2000). Especially, nowadays the consequences of global energy production based on oil and coal can be seen everywhere.

Renewable Energy has often been mentioned together with climate change and because of that reason, it is important to get an understanding of its' definition. It is important to mention the core essence of renewables, which is energy harvested from natural processes that are rejuvenated faster than they are consumed. Contrary to that, the formation of fossil fuels needs several million years (Frewin 2015) (Kanniah 2015).

1.2 Tidal Energy

The motivation for clean and renewable energy resources has pushed the interests of wind and tidal turbines significantly forward. Even though the physics are very similar, both extract energy from a surrounding flow, the focus of this work is on tidal turbines or marine current turbines (MCT). Actually, in a broad sense, tidal energy is another form of hydro energy that can harvest a significant amount of energy due to marine current and ocean tides in order to generate electricity. Usually, most people already heard of hydroelectric energy. This energy production is using a dam to store water in a reservoir and one of the classical hydro turbines, such as Pelton, Francis or Kaplan to convert the potential energy into mechanical energy and finally into electrical energy, however, MCT work differently (Young, Motley and Yeung 2010) (Alternative-Energy-Tutorials 2018).

Tidal turbines can be placed on the seabed in regions where a strong tidal flow is considered. The gravitational influence of the moon and sun in combination with the rotation of the earth causes the tides. In certain locations around the globe, this results in a variation of the water levels close to the shore up to 12 metres. 1000 years ago, in Europe people already used this knowledge to operate grain mills.

Marine current energy is subdivided into tidal energy and wave energy. Contrary to tidal energy wave energy has only recently been started to harvest from ocean waves, with various devices. One of the more common ones is the Pelamis, which is completely different from MCTs (US-EIA 2018).

As already mentioned before, MCTs can be seen as submerged windmills. They even look similar. Due to the significant differences in fluid density, in general water is about 800 times denser than air, tidal turbines have to be much sturdier and heavier than wind turbines. Usually, comparing tidal turbines to onshore wind turbines, the typical operating flow speed of tidal turbines is only about one-sixth of onshore wind turbines, thus the energy density is much higher. Being defined as the energy per unit area, the energy density for the same energy efficiency turbines can be three to four times higher for tidal turbines. It follows that for the same energy ratings the hydrodynamic load on a tidal turbine is also three to four times higher. Since the flow can be considered to be of bidirectional nature, the tidal boundary layer and surface waves also cause the flow to vary spatially and temporally (US-EIA 2018) (Hanania, Stenhouse and Donev 2017).

According to the University of Calgary (Professor Jason Donev), tidal energy is way more reliable than either wind or solar energy due to the fact that there is neither always sun nor wind. It can be foreseen how much electricity the tidal energy source is going to generate at any given time, however tidal energy is still considered intermittent, which means that although it is predictable it still is non-dispatchable. It cannot just be turned on or off like a natural gas power plant. Thus, the predictability of tidal energy can be seen as very attractive to grid management due to the fact that the number of backup power plants can be decreased (Conca 2017).

1.3 State of the Art

Currently, tidal energy production is still at the very beginning. The power produced is still small due to the fact that there are very few MCTs operating worldwide. South Korea has the largest facility at the moment and countries like China, France, England, Canada and Russia have quite some potential to use this type of renewable energy. Contrary in the USA, investors are not very convinced about the tidal energy, due to the fact that there are legal concerns about underwater land ownership, as well as there is no guarantee that the technique is able to gain profit, yet. There are several engineering teams, working on the technology of tidal energy generators first, to increase the amount of energy, they can harvest and secondly, to decrease the environmental impact (GEOGRAPHIC 2018). Finally, for illustration purposes, several two-bladed MCTs are shown in Figure 1, which is printed below.

1.4 Problem Statement & Motivation

MCTs are often exposed to unsteady loadings due to non-uniform and unsteady flow conditions in the stream. These conditions occur due to the variations of the inflow, plus time-dependent inflow conditions cause an unsteady flow field around the blades. The developed field then generates non-steady loads on the turbine blades, resulting in deformation, which in turn affects the flow field. Furthermore, the turbulent boundary-layer flow in the vicinity of the bottom and the free-surface within tidal currents are also contributing to the unsteady load conditions. All the mentioned forces may cause the turbine blades to vibrate, independently of the movement of the turbine itself, meaning it could stand still or rotate (T. B. Clara 2014). Due to the fact that vibration decreases the turbine blades' lifetime by accelerating crack initiation and crack growth, it is very important to investigate into the vibrational behaviour of the turbine blades. It is of huge interest in order to prevent failures due to fatigue plus guarantee structural integrity for extreme load conditions (T. B. Clara 2014).

The considered problem is called a hydroelastic problem and usually involves a complex fluid-structure interaction problem. When designing a turbine, costly methods are required to perform a hydroelastic analysis of the blades, which can be used to optimise the design.

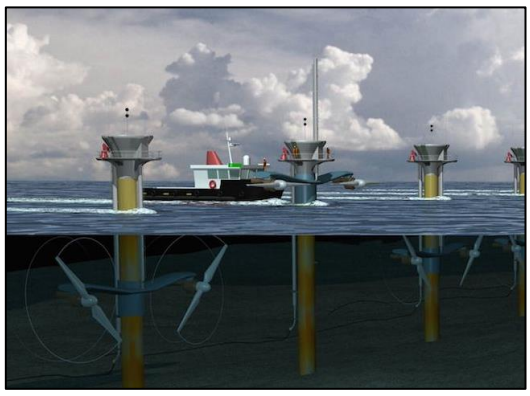

Figure 1: Two-bladed tidal turbine in operation (Conca 2017)

A more simple approach has been presented in Tiago Clara's Master Thesis, where a Boundary Element (BEM) code has been coupled with a code using the Finite Element Method (FEM). The BEM is responsible for computing the added mass and the damping matrices, which are then introduced into the FEM structural mass and damping matrices. With the assumption of small deformations, the usual approach for undertaking the structural vibrational analysis with the FEM code has been performed. Contrary to Young's scientific papers (*Time-dependent hydroelastic analysis of cavitating propulsors* and *three-dimensional numerical modelling of the transient fluid-structural interaction response of tidal turbines*), who used Abaqus, the eigenmode analysis has been executed in Ansys, whereas the added mass matrices have been computed with an in-house BEM code (Clara, Falcão de Campos and Baltazar 2015).

The problem which occurred is, that Clara could not reach an agreement with Young's results in her papers. Even though Clara's methodology seems to work, when he was introducing his model to simple structures, there is a disagreement compared to Young's paper.

It was now of great interest to repeat the calculations for the same blade with the difference of using Abaqus as a FEM software instead of ANSYS. Furthermore, the approach in this work also aims for a fundamental investigation of the methodology due to the fact that Clara already discovered some problems for simple structures.

1.5 Natural Frequency

The most important parameter for a free vibrating system, which means, without any force, clear, is the natural frequency. In principle, the natural frequency for an undamped system is only dependent on the stiffness of the system, which further on depends on the mode shape and the mass of the system. However, if the system is submerged, as it is the case with MCT, the so-called added mass effect plays a dominant role, and therefore it is unavoidable to figure out how to compute the added mass, even for complex structures, like a twisted blade of an MCT.

1.6 Content & Structure

The paper consists of four chapters, whereas this one, the introduction deals with a general introduction to the topic and sets the performed work into a broader framework. In chapter II the theory of computing natural frequencies for certain structures is explained, as well as the added mass effect and the differences between T. Clara, Young and this work. The methodology and explanation for using Abaqus are presented in Chapter III, as well as the results. Finally, some conclusions are drawn in Chapter IV. A list of references follows Chapter IV, as well as a table of accumulated results in the annexe.

2. THEORY

2.1 Beam Flexure: Elementary Case

The first step of the general approach to the dynamic response analysis of a distributed-parameter system would be the evaluation of its undamped-vibration mode shapes and frequencies. As a reminder, this is exactly what is needed for the analysis of the marine current turbine. For the sake of simplicity the considered cases are restricted to beams with uniform properties alongside their length or to structures that are assemblies made out of such rectangular members.

Consideration of the elementary case, neglecting shear distortions and rotatory inertia and assuming that the axial-force effects are also negligible the equation of motion for the free vibrations of a rectangular beam can be formulated as

$$EI\frac{\partial^4 v}{\partial x^4} + \bar{m}\frac{\partial^2 v}{\partial t^2} = 0 \qquad (1)$$

After dividing the term above by EI, the product of Young's Modulus E and the second moment of Area I and using different indications for different differentiation, which is primes for the ones with respect to the location x and dots for the ones with respect to the time t the whole equation gets

$$v^{iv} + \frac{\bar{m}}{EI}\ddot{v} = 0 \qquad (2)$$

The letter v indicates a displacement response. Performing a separation of variables for (2) is one tool to solve the equation. The solution would have a form like (3)

$$v(x,t) = \phi(x)Y(t) \qquad (3)$$

Trying to formulate (3) in words, would be, that it is assumed, that the free-vibration motion consists of a constant shape $\phi(x)$ having a time-varying amplitude, expressed with the term $Y(t)$. Taking the last two equations and substituting the lower in the upper one, derives the expression (4)

$$\phi^{iv}(x)Y(t) + \frac{\bar{m}}{EI}\phi(x)\ddot{Y}(t) = 0, \qquad (4)$$

which is then divided by $\phi(x)Y(t)$ in order to achieve the desired separation of variables. It follows that (4) derives to (5), written as

$$\frac{\phi^{iv}(x)}{\phi(x)} + \frac{\bar{m}}{EI}\frac{\ddot{Y}(t)}{Y(t)} = 0 \qquad (5)$$

Due to the fact that in (5) the first term is only depended on x whereas the second term is only dependent on the time t, the whole equation can be fulfilled by a random x and t only if each term is equal to constant, so it follows that

$$\frac{\phi^{iv}(x)}{\phi(x)} = \bar{C} = -\frac{\bar{m}}{EI}\frac{\ddot{Y}(t)}{Y(t)} \qquad (6)$$

Choosing the constant $\bar{C}$ conveniently as a polynomial of 4th order, like a^4, the two differential equation can be written as follows

$$\phi^{iv}(x) - a^4\phi(x) = 0 \qquad (7)$$

and

$$\ddot{Y}(t) + \omega^2 Y(t) = 0 \qquad (8)$$

Here, it has to be announced that

$$a^4 = \frac{\omega^2\bar{m}}{EI} \qquad (9)$$

or

$$\omega^2 = \frac{a^4 EI}{\bar{m}} \qquad (10)$$

are equally valid.

The second of the differential equation is really easy to solve due to the fact that this the already very well-known free-vibration equation for an undamped SDOF system, which has the following solution

$$Y(t) = A\sin\omega t + B\cos\omega t \qquad (11)$$

The constants A and B depend upon the initial conditions, namely the initial velocity as well as the initial displacement. These can then be substituted into the equation and that gives

$$Y(t) = \frac{\dot{Y}(0)}{\omega}\sin\omega t + Y(0)\cos\omega t \qquad (12)$$

The other differential equation can be solved following a solution in the form of

$$\phi(x) = Ce^{sx} \qquad (13)$$

The equation now gets

$$(s^4 - a^4)Ce^{sx} = 0 \qquad (14)$$

from which it follows that

$$s = \pm a, \pm ia \qquad (15)$$

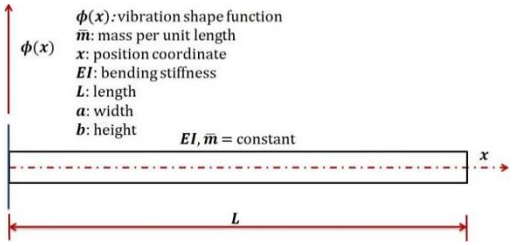

Figure 2: Cantilever-beam vibration analysis (Clough and Penzien 1975)

The solution then is

$$\phi(x) = C_1 e^{iax} + C_2 e^{-iax} + C_3 e^{ax} + C_4 e^{-ax} \qquad (16)$$

The ends of any given beam segments are very crucial for determining the four constants C_n included in the equation above. They define the shape and amplitude of the beam vibration and are dependent on the boundary conditions (BC).

At each end of the beam segments, two conditions should express displacement, slope, moment or shear force. Three out of four constant can be found and then be expressed in terms of the fourth. The derived expression is the so-called frequency equation, which is necessary to evaluate the frequency parameter a. The remaining constant defines the amplitude of motion, which is dependent on the initial conditions and can therefore not be computed directly in the free vibration analysis.

Using the knowledge gained, an example is provided. An investigation in the cantilever beam has been done, which can be seen in Figure 2.

Compared to the simple beam, where only one term of the shape function expresses the mode shapes, the solution of the cantilever beam is rather complex. The four BCs for the cantilever are as follows; at $x = 0$ it is valid, that

$$\phi(0) = 0 \; and \; \phi'(0) = 0, \qquad (17)$$

and at $x = L$ it is valid that

$$\mathcal{M} = EI\phi''(L) = 0 \; and \; v = EI\phi'''(L) = 0 \qquad (18)$$

Using these BC equations finally lead to an expression for a, which is

$$1 + \cos aL + \cosh aL = 0 \qquad (19)$$

It can be seen easily, that no analytical solution exists for the equation above and that is the reason why it has to be solved numerically. However, the solutions provide the values of aL which represent the frequencies of vibration of the cantilever beam. It should be reminded here, that there is per definition an expression for a

$$a^4 = \frac{\omega^2\bar{m}}{EI} \qquad (20)$$

which leads to an equal expression

$$\omega^2 = a^4\frac{EI}{\bar{m}} \qquad (21)$$

If the modal values are gained from the frequency equation, they can be inserted in the expressions for the shape-function of the cantilever beam in order to obtain the corresponding mode shapes.

$$\phi(x) = A_1\left[\sin ax - \sinh ax + \frac{\sin aL + \sinh aL}{\cos aL + \cosh aL}(\cosh ax - \cos ax)\right] \qquad (22)$$

Coming back to the expression for the frequency equation, this can also be written, as follows

$$1 + \cos x + \cosh x = 0 \tag{23}$$

and given a substitution

$$x = aL \text{ as well as } x^4 = a^4 L^4 \tag{24}$$

which finally provides

$$\omega^2 = \frac{x^4}{L^4}\frac{EI}{\bar{m}} \tag{25}$$

$$\omega = x^2 \sqrt{\frac{EI}{\bar{m}L^4}} \tag{26}$$

If now, for the sake of completeness the first four solutions for the frequency equation are given with the help of a numerical approximation it follows that

$$a^4 L^4 = x^4 = 1.875 \tag{27}$$

$$a^4 L^4 = x^4 = 4.694 \tag{28}$$

$$a^4 L^4 = x^4 = 7.855 \tag{29}$$

$$a^4 L^4 = x^4 = 10.99 \tag{30}$$

and finally the first four bending modes can be evaluated, as well as the first four natural frequencies are approximately given by (31,32,33,34):

$$\omega_1 = (1.875)^2 \sqrt{\frac{EI}{\bar{m}L^4}} \tag{31}$$

$$\omega_2 = (4.694)^2 \sqrt{\frac{EI}{\bar{m}L^4}} \tag{32}$$

$$\omega_3 = (7.855)^2 \sqrt{\frac{EI}{\bar{m}L^4}} \tag{33}$$

$$\omega_4 = (10.99)^2 \sqrt{\frac{EI}{\bar{m}L^4}} \tag{34}$$

Summarizing, the first four mode shapes can be seen in Figure 3. Starting from the very left, the figure shows the first vibration mode shape, continuing with the second, the third and finally the fourth mode shape can be seen on the very right. The corresponding formulas for the first four natural frequencies were presented above (Clough and Penzien 1975).

However, it has to be noted, that this formula is only valid for pure bending modes or at least that this formula does not take any other effects into account. The axial force effects are neglected here, due to the fact that these will not be important for the marine current turbine. However, the following paragraphs deal with including shear deformation and rotatory inertia.

2.2 Including Shear Deformations and Rotatory Inertia

In the preceding section, the equation of motion for the transverse vibration of a simple and cantilever beam has been developed, excluding the inertial moment linked with the rotation of the beam sections. The only deflections included in these equations were the ones associated with bending stresses, no consideration of the deflection coming from shear stresses have been made for the beam. Both effects, rotational inertia and shear deformation are considered in the following paragraphs, according to the *Timoshenko Beam Theory*.

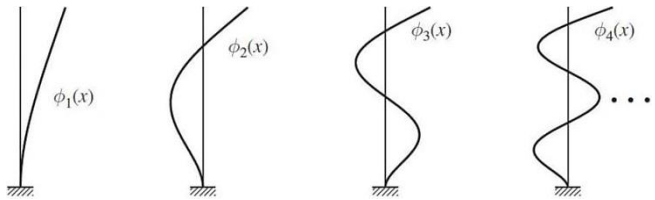

Figure 3: Cantilever-beam vibration analysis, first four vibration mode shapes (Chopra 2012)

Recalling the equation which describes the free vibrations of a uniform beam with $m(x) = m$ as well as $EI(x) = EI$ is

$$EI\frac{\partial^4 v}{\partial x^4} - \left(p - \bar{m}\frac{\partial^2 v}{\partial t^2}\right) - \bar{m}r^2\frac{\partial^4 v}{\partial x^2 \partial t^2} + \frac{EI}{k'AG}\frac{\partial^2}{\partial x^2}\left(p - \bar{m}\frac{\partial^2 v}{\partial t^2}\right) - \frac{\bar{m}r^2}{k'AG}\frac{\partial}{\partial t^2}\left(p - \bar{m}\frac{\partial^2 v}{\partial t^2}\right) = 0 \tag{35}$$

As a reminder, r is the radius of gyration and depended and the second moment of area I and the cross sectional area A, whereas G describes the shear modulus. The constant k' can be looked up from different tables in other solid mechanic text books.

Including the earlier-mentioned effects can be seen easily as a correction factor of the already derived formula for a cantilever beam excluding these effects. Therefore, as a first step, investigation of a beam with both ends simply supported is done. The assumed solution has the form of

$$v(x,t) = C \sin\left(\frac{n\pi x}{L}\right) \sin \omega_n' t \tag{36}$$

which satisfies the necessary end conditions.

The following convention is introduced for describing a natural frequency of the beam with ω_n', if shear and rotational inertia effects are included and ω_n if these effects are excluded. Now, defining

$$\Omega_n = \frac{\omega_n'}{\omega_n} \tag{37}$$

the frequency equation can be rewritten as

$$(1 - \Omega_n^2) - \Omega_n^2 \left(\frac{n\pi r}{L}\right)^2 \left(1 + \frac{E}{k'G}\right) + \Omega_n^4 \left(\frac{n\pi r}{L}\right)^4 \frac{E}{k'G} = 0 \tag{38}$$

If the following assumption, that $nr/L \ll 1$ is valid, the last term of the equation might be dropped and the whole equation is reduced to

$$\omega_n' = \omega_n \frac{1}{\sqrt{1 + \left(\frac{n\pi r}{L}\right)^2 \left(1 + \frac{E}{k'G}\right)}} \tag{39}$$

It can be seen easily, that $\omega_n' < \omega_n$ is valid. As mentioned earlier on, including rotational inertia and shear deformation can be seen as correction factors and exactly this is represented in the equation above. Thus, the correction coming from rotational inertia is represented by $\left(\frac{n\pi r}{L}\right)^2$ in the denominator, whereas the shear deformation is the multiplication of $\left(\frac{n\pi r}{L}\right)^2 \left(\frac{E}{k'G}\right)$.

It follows that the correction influence of shear deformation is exactly $E/k'G$ times larger than the rotational influence term. Both, shear deformation and rotational inertia have the effect of lowering the natural frequencies. Further on, given a fixed relation of length over radius of gyration, the so-called slenderness ratio of the beam, the frequency reduction caused by the shear deformation and rotational inertia increases for larger $E/k'G$ values and also with the mode number. In other words, this means that the correction factors including shear deformation and rotational inertia might be not as important in the fundamental modes as they are for higher modes.

Furthermore, within the same mode as well as with a fixed value of $E/k'G$ the influence of the correction factor increases, when the ratio r over L increases.

It can be concluded that the reduction factors are more important for less slender and thicker beams. Usually, the analysis itself should give a clear picture of whether these corrections would play a significant role or not. This is motivated by two examples. The response analysis of earthquakes for many structures do not need the correction factors, however, it should, not be forgotten that they, exist. On the other hand, they might get important for an FE formulation for some structures which are not accessible to solutions as infinite-DOF systems (Chopra 2012).

Coming back to the formula, which has been derived on the previous page, inserting every term would give

$$\omega_n^{air} = x^2 \sqrt{\frac{EI}{\bar{m}L^4}} \frac{1}{\sqrt{1+\left(\frac{n\pi r}{L}\right)^2\left(1+\frac{E}{k'G}\right)}} \qquad (40)$$

as it is similarly mentioned in Young's Paper, *Time-dependent hydroelastic analysis of cavitating propulsors* (Y. J. Young 2006).

2.3 Free Vibrations in Torsion

Another important final formula that is later on used for the analytical solution of natural frequencies of simple geometries, is the formula for free undamped vibrations in torsion for a cantilever beam. Previously, the formula for free vibrations in axial deformations has been derived, which looks, mathematically seen quite similar to the following formula

$$\omega_n = \frac{2n-1}{2}\pi\sqrt{\frac{Gk}{\bar{J}L^2}} \qquad (41)$$

It also has the prefix $\frac{2n-1}{2}\pi$, where n refers to the mode number. The elastic constant here is now the shear modulus G instead of the Young's Modulus E. Furthermore $\bar{J}$ describes the moment of inertia per unit length and k (caution, not to confuse with k' as an influence factor) is the torsion coefficient. Both mentioned factors are depended on the geometry of the cross section (Faria 2018).

2.4 Fluid-Structure Interaction

The fluid-structure interaction (FSI) deals with the coupled dynamics of structures, which are in contact with a fluid.

Exactly this is the case for the MCT blade. Figure 4 basically shows the ongoing circle of interactions. Describing the Figure 4 in words would be that the movements of the present structure influence the flow conditions at the interface with the fluid, which then, in turn, is responsible for a change in the pressure and/or viscous forces. Further on this has an influence on the applied loading to the fluid-structure interface and therefore changes the motion of the given structure.

A usual approach for modelling FSI is that both, the structure and the fluid particles of a coupled system are analysed within the framework of the continuum mechanics. From the knowledge gained above, it is quite clear now that the motions are described by partial differential equations in combination with BCs. However, in some circumstances, it could be easier to formulate the differential equations of the fluid motion as integrals (Sigrist 2015).

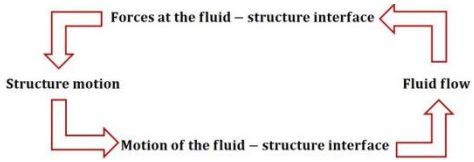

Figure 4: FSI interaction, coupling mechanism (Sigrist 2015)

2.5 The added mass effect

In general, the added mass effect has to be considered for the case of unsteady motions of submerged bodies or if unsteady flow around an object occurs. The additional effect *(or force)* which results from the fluid attacking the structure in water has to be considered when formulating the equations of motions for that particular system. Contrary, in air the effect also exits but as a reminder here, the density of air is about 800 times lighter than water (compared at 20°C and 1013mbar), which concludes that most of the times this effect in air is negligible.

Describing the added mass within the framework of a physical signification, it is the weight added to a system. This results from an either accelerating or decelerating body (so to say an unsteady motion $dv/dt \neq 0$), which has to take some volume of its surrounding fluid with it as it moves. For example, if a ship heaves upwards in the waves, water will flow to the spot, where the ship has been just one moment ago and the wetted surface of the ship will drag water with it, which then can be seen as added inertia. The added mass force works against the motion of the submerged structure and therefore can be factored in the system equation. Due to the fact that the derivation would go a bit beyond the scope of the work, only the necessary equations are presented.

Coming back to the equation of motion of a system, including the added mass effect, this can be expressed as follows:

$$(m + m_a)\ddot{v} + kv = 0 \qquad (42)$$

the mass m and the added mass m_a can be summarised as m'. Hence, the natural frequency could be formulated as

$$\omega' = \sqrt{\frac{k}{m'}} = \sqrt{\frac{k}{m+m_a}} \qquad (43)$$

Now, linking back to (45) which is valid for undamped free vibrations in vacuum/air, including rotatory inertia and shear deformation, an improvement can be made, in order to use this formula also for submerged structures.

Coming from the natural frequencies in air

$$\omega_n^{air} = x^2 \sqrt{\frac{EI}{\bar{m}L^4}} \frac{1}{\sqrt{1+\left(\frac{n\pi r}{L}\right)^2\left(1+\frac{E}{k'G}\right)}} \qquad (44)$$

to the natural frequencies in water, including the added mass

$$\omega_n^{water} = \frac{x^2}{L^2} \sqrt{\frac{EI}{\bar{m}+m_a}} \frac{1}{\sqrt{1+\left(\frac{n\pi r}{L}\right)^2\left(1+\frac{E}{k'G}\right)}} \qquad (45)$$

and knowing that the mass per unit length $\bar{m}$ is expressed as

$$\bar{m} = \rho A \qquad (46)$$

the formula for bending around the abscise can be written as follows (using the Newman added mass coefficients)

$$\omega_n^{water} = \frac{x^2}{L^2} \sqrt{\frac{EI}{\rho_S A + \pi\rho_F a^2}} \frac{1}{\sqrt{1+\left(\frac{n\pi r}{L}\right)^2\left(1+\frac{E}{k'G}\right)}} \qquad (47)$$

whereas ρ_S describes the density of the solid structure and ρ_F describes the density of the fluid domain. The same procedure may be used to include the added mass effects for torsional mode shapes.

Coming from

$$\omega_n = \frac{2n-1}{2}\pi\sqrt{\frac{Gk}{\bar{J}L^2}} \qquad (48)$$

excluding added mass effects, the following formula, including added mass can be concluded

$$\omega_n = \frac{2n-1}{2}\pi\sqrt{\frac{Gk}{(\bar{J}+m_a)L^2}} \qquad (49)$$

2.6 Dissociation from Tiago Clara and Yin Lu Julie Young

Contrary to Tiago Clara and Young, a broad investigation of different meshing techniques has been performed. The validation study of different elements and different mesh sizes has been performed way more elaborated than in the two former ones. Still, both have been used as comparison parameter. In Young's Paper, an analytical formula for the torsional mode shape is missing, which has been presented in this work, whereas Tiago Clara in general only compared with Young, even though, he was also introducing the formula for natural frequencies according to bending modes. Young explains that the natural frequencies for analytical and numerical frequencies are matching for the first two modes and they would not for higher modes due to the fact of the inability of the beam theory for twisting foils. This is partially true; yes, the analytical bending formula cannot be used for twisting, however, an analytical formula for torsional mode does exist, which has been indeed used in this work.

For Tiago Clara, the meshing technique has been applied outside of Ansys, whereas in this work, the meshing has been done with the pre-processor of the software Abaqus, whereas manual partitioning has been applied, where needed.

Furthermore, neither Tiago Clara nor Young did really refine the mesh through the thickness; Young only did it for one element. Also, the added strip theory probably needs to be adjusted for the torsional mode. Furthermore, the lab results from MacBain did not only contain results for twisted structures but also for plates without twist. These *regular plates* results have been used in order to evaluate a general difference in MacBain and analytical formulas.

Finally, Tiago Clara decided to simulate the MCT with one element and did not start a convergence study, which contrary, has been done in this work.

3. METHODS AND RESULTS

3.1 Explanation for operating Abaqus for natural frequencies in water

Determining the natural frequencies of a submerged structure is more complex than determining them in vacuum/air due to the already discussed added mass effect. In Abaqus, it is possible to perform an acoustic analysis which uses one of the dynamic procedures. It could be either just used alone to study the natural frequency of the acoustic domain itself or being coupled with a structural analysis. For this type of analysis the so-called *acoustic elements* are needed and furthermore, for coupled acoustic-structural analysis, a surface-based interaction using tie constraints is required. It could be either used to model an interior problem, where a structure surrounds one or more acoustic cavities or an exterior problem, where a structure is located in a fluid medium extending to infinity. The latter one is exactly the case for the MCT.

In Abaqus, it is possible to introduce a fluid domain, which is assumed to be inviscid and incompressible. It is now important to introduce one more material, the water, or to be even more precise, the sea water. For acoustic elements, there are only two material properties needed, the density and the bulk modulus.

3.2 The water bomb method

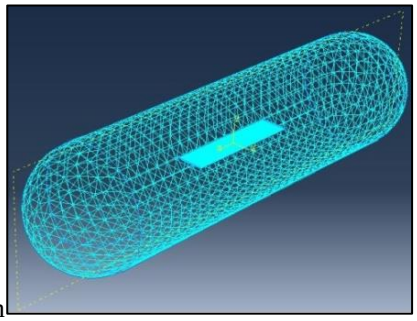

m

Figure 5: Water bomb with the cantilever plate, elliptical cross-section inside

In the part module, a new part is created, which is supposed to be much larger than the structural part. Actually, the water domain should be infinity; however, this is not possible to model, unless infinite elements are used. However, acoustic elements are still needed in order to model the water. Both, the water domain and the structural part are introduced into the assembly module, whereas the structural part is placed centred into the fluid domain. The earlier on mentioned cut option is used in order to cut a hole, which has exactly the same shape as the structural part into the fluid domain. A new part has been created from this cutting option; it could be seen as a water domain, which basically now has a hole.

Again, the structural part is introduced into the assembly module; however, this time the cut water domain is introduced. The structural part is supposed to be exactly placed into the hole of the fluid domain to get later on tied together as a surface to surface based tie constraint inside the interaction module. The tie constraint is responsible to couple the motion of the structural part together with the fluid, or to be more precise, the acoustic elements to the solid elements, in order to be able to get the aimed added mass effect. Several options for the tie constraint are shown in At this point, it has to be emphasized once more, that the option of including acoustic-structural coupling should be activated inside the step module when editing the step itself.

The method has been evaluated on a simple structure; the CPECS has been introduced into a water domain, due to the fact that the simulated values can be compared with results from Young, as well as using the 2D added mass coefficients from Newman. The water bomb can be seen in Figure 5 and a view cut which shows the CPECS inside the water domain, coloured in green is illustrated in Figure 6.

A comparison between the FEM simulations and the 2D added mass theory has been done, which is presented in Appendix Table 1. The formulas, which have been used for the analytical part have been presented in chapter II, the natural frequencies including the added mass effect with the help of the tabulated Newman's added mass coefficients. It should be clear, that the contribution of the added mass in the analytical formula stays the same for every mode, which is clearly not the case for real structures. The influence of the water on lower modes is higher due to its mode shape and declines for higher modes. This is the reason why the error function in Appendix Table 1gets larger for higher modes.

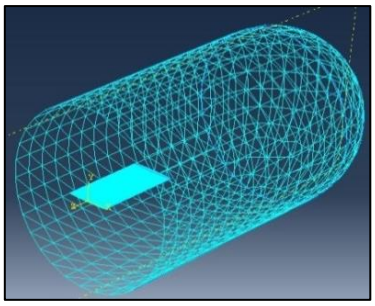

Figure 6: Cut through the water bomb with the cantilever plate, elliptical cross-section inside, indicated in green (middle)

However, the table shows that the results obtained in the FEM are not completely off from the analytical ones. Here it should be clearly stated, that the aim of this investigation should give a rough estimation, due to the fact that the applied strip theory for the analytical solutions work with high approximations and as already indicated have the same contribution of the added mass for every mode, because the added mass coefficient stays the same. To underline this statement, even more, Table 1 also presents the FEM compared to the analytical results in air, which according to the error function are very close to each other.

3.3 Natural Frequencies of the MCT blade

The investigation into the blade profile were one, three, ten and thirty elements over the thickness also taking into account linear brick and quadratic brick elements. Due to the complexness of the geometry of the MCT blade, the blade is twisted with an angle of 30 degrees alongside the span, as well as the cross-sectional area decreases from the hub to tip, the choice of meshing is more restricted and not as free as it has been for the simple structures. The smaller ends of the quasi-elliptical shape are usually meshed using the triangular prism elements, whereas the rest of the part has been meshed with brick elements. It was expected to gain similar behaviour as before with the simple geometries when using only one linear reduced integration element (C3D8R for example) over the thickness.

Figure 7, Figure 8, Figure 9 are presenting mode number 1, 2 and 3 respectively in air for five different meshing techniques. Mesh number 1 to mesh number 4 refers to meshes consisting of both, C3D8R in the centre and C3D6 elements at the tips of the ellipsis, whereas for mesh number 5 it has been tried to only use C3D6 elements, which apparently is not a great idea. It is remarkable, that for these graphs the quadratic elements are relatively stable and show the same behaviour and always converge towards the same results. Concerning the linear elements, at least two have to be placed over the thickness for gained better results at least for mode number 1. For mode number 2 and 3, the linear meshes 2, 3 and 4 are slightly drifting away from their quadratic equivalent meshes, however, mesh number 4 always seems to be quite stable.

Table 1: Comparison between the water bomb method and the 2D added mass theory

Mode	ω in air [Hz]	Analytical in air [Hz]	Error function [%]	ω in water [Hz]	Analytical in water[Hz]	Error function [%]
1B	17.974	17.73	1.36	6.8801	6.214	9.68
2B	112.15	111.008	1.02	44.386	38.927	12.30
3B	312.6	310.812	0.57	130.5	108.92	16.54
4B	609.01	608.464	0.09	271.52	213.229	21.47

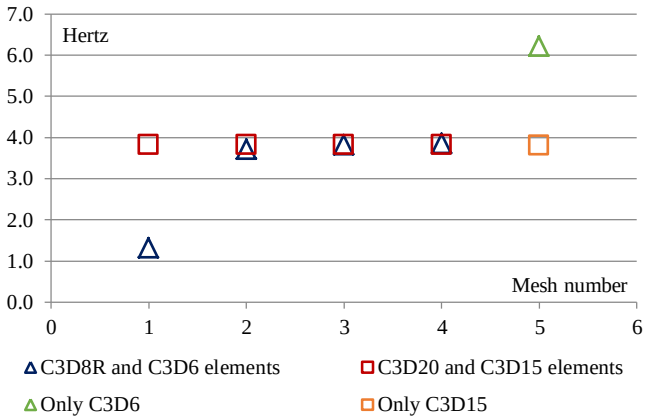

Figure 7: Mode #1 of the MCT blade in air with 10 different meshes

The same approach for different meshing techniques has been done for the blade in water using the earlier on explained water bomb method. Figure 10, Figure 11 and Figure 12 are showing the results for the first three modes of the MCT blade in water using four different meshing techniques. Also, the acoustic elements can either be used linear namely AC3D4 or quadratic namely AC3D10 elements. Unfortunately, the computations for mesh number 5 in water were too large for the operating machine. Even though, using all the available power the time for calculations usually exceeded one day due to the fact that the water domain contributes with a lot of elements as well. However, the remaining four meshes have been evaluated to be enough for confidently arguing, that the water bomb method shows convergence, especially for the quadratic elements.

In a comparison between the results obtained in this work and Tiago Clara's as well as Young's results has been done. It is quite strange to witness the convergence towards the third mode for all comparisons. Usually, the higher the mode numbers, the less different approaches even show convergence. Furthermore, it gets clear, that Young must have used a different approach due to the fact, that already the natural frequencies in air are quite different from the one obtained in this work. If only the natural frequencies in water would have been different, then the bombing method could have been questioned, however both in air and water are far away from Young's result, especially in the first modes.

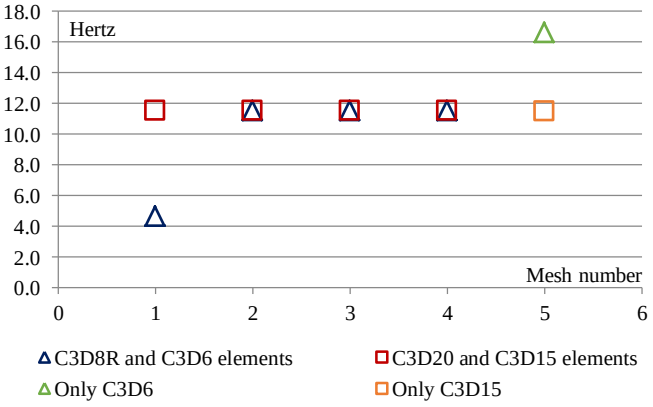

Figure 8: Mode #2 of the MCT blade in air with 10 different meshes

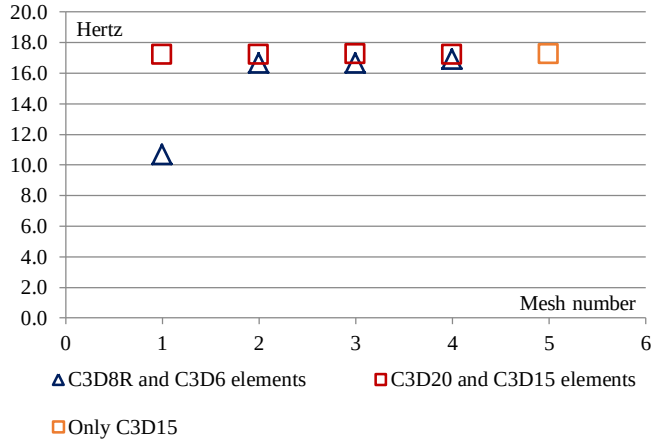

Figure 9: Mode #3 of the MCT blade in air with 9 different meshes

In Appendix Table 1 a comparison between the results obtained in this work and Tiago Clara's as well as Young's results has been done. It is quite strange to witness the convergence towards the third mode for all comparisons. Usually, the higher the mode numbers, the less different approaches even show convergence. Furthermore, it gets clear, that Young must have used a different approach due to the fact, that already the natural frequencies in air are quite different from the one obtained in this work. If only the natural frequencies in water would have been different, then the bombing method could have been questioned, however both in air and water are far away from Young's result, especially in the first modes.

For meshes, which have been considered to be quite accurate the results are never more than 5% different from the results obtained by Tiago Clara, in general. Obviously, the linear reduced elements with only one element over thickness are terribly wrong, but going further down in Appendix Table 1 it can be seen that there is a strong agreement with the results from Tiago Clara's master thesis, especially comparing the natural frequencies in air. These results do not differentiate from the previous work by more than 1%.

The type of elements does not have an influence on the mode shape, as well as it does not make a difference whether the blade is in vacuum/air or water.

4 Conclusions

Recalling Chapter III, it started off with describing the differences between this work and previous works from Tiago Clara and Yin Lu Julie Young. At this point, it has to be emphasized once more, that in the other two works a formula for twisting modes is missing, it has not been introduced or used for comparison between analytical and simulated results. Here a clear differentiation between bending and torsional mode shapes has been undertaken. Furthermore, depending on the used boundary condition (totally clamped or a different approach) it was possible to simulate very accurate results for the torsional mode using shell elements and allowing the effect of warping.

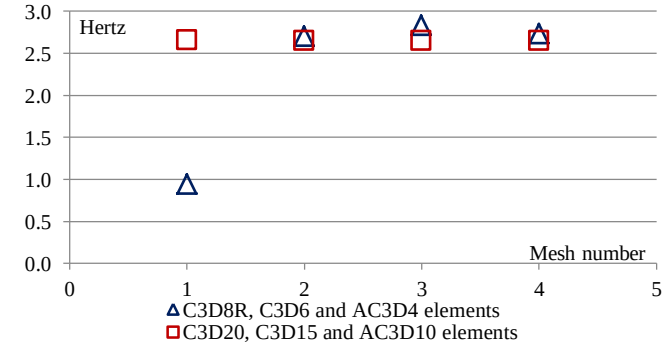

Figure 10: Mode #1 of the MCT blade in water with 8 different meshes

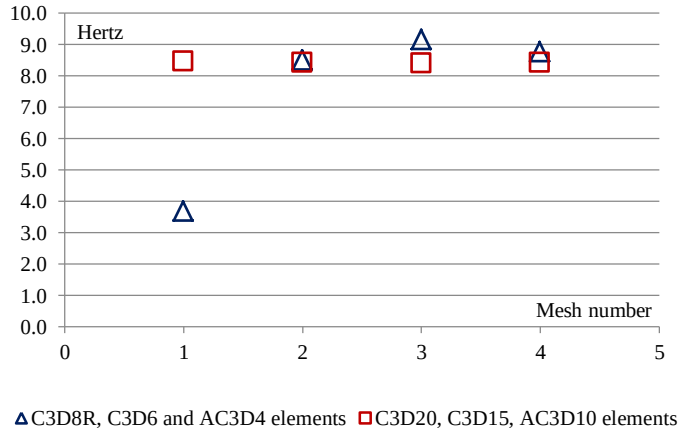

Figure 11: Mode #2 of the MCT blade in water with 8 different meshes

Another important aspect was to ensure a good mesh quality and mesh control and that is why the meshing itself has been performed in the same software, which was responsible for calculating the natural frequencies and simulating the mode shapes. No external coding has been used, which potentially could lead to a source of errors.

The work also shows that it has been understood which options in the meshing module need to be chosen for comparison with which analytical formula. In particular, for one-dimensional elements, the options of shear-flexible and cubic formulation have been presented and it has been explained why one of the options is superior to the other one. For example, if an analytical formula is used which does not take shear deformation and rotatory inertia into account a specific set of parameters in Abaqus needs to be activated in order to able to obtain good results, which then can be compared to the analytical ones.

It followed that for the beam in 2D planar as well as in 3D space the simulation results were in good agreement with the analytical results and therefore can be classified as correct.

One step further, concerning shell elements the earlier on mentioned formula for torsional modes has been used and showed an error of around 8% in the worst cases. The bending modes again were in very good agreement with the analytical results with 1.5% at its worst and therefore can also be classified as being correctly simulated. It has been found out, that the BCs were responsible for larger error for twisting modes as it did not allow warping. Changing BC also made it possible to converge to very good results for the torsional mode of 0.5% for suitable elements. However, the only downgrade was that with the change of the BC the results of the bending modes were far off. Still, it can be concluded that with the implementation of the correct BC it is possible to simulate correct results which are in accordance with the analytical ones for bending as well as for torsional modes.

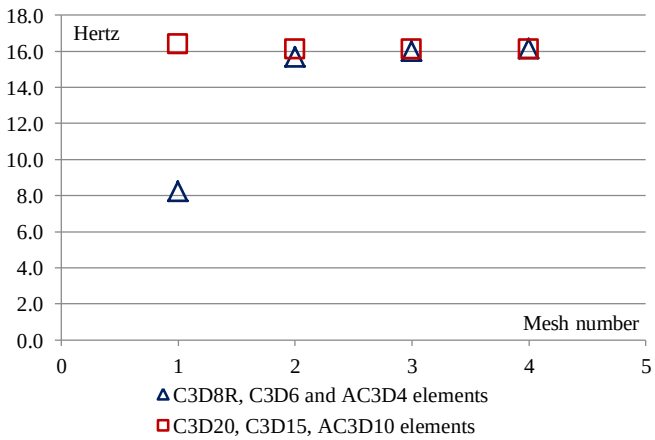

Figure 12: Mode #3 of the MCT blade in water with 8 different meshes

Looking at the 3D elements, it can be concluded that it is very crucial to use certain types of elements if only one element over the thickness is used. However, even elements which do not show a correct behaviour are able to produce good results, if the amount of elements over the thickness is increased. However, this conclusion is valid for the CPRCS and CPECS. For the geometry, which includes twist, CPT respectively this behaviour cannot be exactly observed. It shares the fact with the first two mentioned geometries, that good results depend on the element type, however, some of the simulated results are actually drifting further away, if more elements through the thickness are used. For instance, C3D6 and C3D6H are producing good results, taking into account that mode number three is the torsion mode and therefore further off, however, if the number of these elements is increased over the thickness the values are further away from MacBain's experimental investigation. Nonetheless having a closer look at the third mesh, which as a reminder was four elements over the thickness, most element types converge to common results. For mode number one this is around 90 Hz, for mode number 2 around 504 Hz, for mode number 3 around 665 Hz and for mode number four around 1481 Hz.

Hence, it definitely can be concluded that meshing is a very crucial factor, especially since the MCT blade is a combination of the CPECS and CPT and both geometries separated had to be treated differently.

In Appendix Table 1 comparison between the results obtained in this work and Tiago Clara's as well as Young's results has been done. It is quite strange to witness the convergence towards the third mode for all comparisons. Usually, the higher the mode numbers, the less different approaches even show convergence. Furthermore, it gets clear, that Young must have used a different approach due to the fact, that already the natural frequencies in air are quite different from the one obtained in this work. If only the natural frequencies in water would have been different, then the bombing method could have been questioned, however both in air and water are far away from Young's result, especially in the first modes. For meshes, which have been considered to be quite accurate the results are never more than 5% different from the results obtained by Tiago Clara, in general. Obviously, the linear reduced elements with only one element over thickness are terribly wrong, but going further down in Appendix Table 1 it can be seen that there is a strong agreement with the results from Tiago Clara's master thesis, especially comparing the natural frequencies in air. These results do not differentiate from the previous work by more than 1%.The type of elements does not have an influence on the mode shape, as well as it does not make a difference whether the blade is in vacuum/air or water. Finally, it can be concluded, that implementing the added mass effect for MCT is rather complex but at the same time a very crucial and important step. The mode shapes stay the same, however, the natural frequencies are drastically reduced due to the discussed added mass effect. With the help of the simple geometries, it has been evaluated, that Abaqus works precise and close enough to the analytical solutions. Furthermore, the importance of using certain types of elements as well as several elements over the thickness of the cross-sectional area has been identified and further on used for the MCT. However, applying the methods to a very complex structure like the MCT is quite a bit different. Even though the results of the natural frequency itself converge, there are remarkable differences to the literature, or better say to Young's Paper. The results are different for both natural frequencies in air and water. Especially interesting is the fact that the results are getting closer to each other in higher modes.

It can be concluded that Young is taking parts of the hub into account, due to two facts, first, her results are lower than both the ones of Tiago Clara as well as the results of this work and secondly there is a detailed drawing in one of her papers, especially showing the hub. From the presented graphs in this work, it can be seen that the results again are very dependent on the mesh, the same way as they have been very dependent on the mesh for the simple structures. However, using the right meshing technique and a proper amount of element over the thickness gives confidence about the convergence of the applied methods. Nevertheless, it can be stated that the results are usable because they are aligned with Clara's work. His argumentation of not getting the same results as Young, using a different FEM software is hereby invalid, due to the fact that with Abaqus it was possible to show that Clara's results cannot be very wrong, the only might be slightly off because no investigation in a convergence study has been done.

It has been shown that independent methods of Clara and this work do show similar results, which is quite remarkable.

ACKNOWLEDGEMENT

First of all, I would like to express my thankfulness to Luis Faria, who has supported me throughout the thesis with books, scientific papers, his knowledge and the countless discussion rounds about natural frequencies, structural vibrations and how to deal with finite element problems. Furthermore, for his frequent support even over the hot summer of Lisbon. Also thanks for being there from the first discussion until the thesis defence. The discussion rounds have also been frequently completed by Falcão de Campos, who I would like to say special thanks for proposing the topic of this thesis and finally the trust in me of solving the problems. Also thanks for being a supportive MEGE coordinator.

Also special thanks to Jorge Matos as my ENTECH course coordinator and contribution to be the chairman of the Jury. Further thanks for the discussion throughout my studies in Lisbon.

Thanks to Luis Sousa for being a great support for SolidWorks and giving my hands on how to deal with the program and his idea how to set up a geometry model for the turbine blade. Also thanks for being part of the Jury.

Thanks to Carlos Quental, who has provided me with all kind of help for installing the required software and his knowledge of Abaqus and SolidWorks. Thank you for being able to drop by your office at any time, I needed to. Also thanks to João Baltazar who has provided me with the geometry data of the turbine.

Thank you all very much.

REFERENCES

Alternative-Energy-Tutorials. *Tidal Energy, Using the Energy of Tides to Generate Electricity.* 1st August 2018. http://www.alternative-energy-tutorials.com/tidal-energy/tidal-energy.html (accessed August 31st, 2018).

Baltazar, João. "Dynamics of Marine Structures II." *OWE Lecture 17.* Lisbon, Lisbon: University of Lisbon, 22nd November 2017.

Chandler, Hugo. *Empowering Variable Renewables - Options for Flexible Electricity Systems.* Task requested by G8 Summit, Paris: International Energy Agency, 2008.

Chopra, Anil K. *Dynamics of Structures - Theory and Applications to Earthquake Engineering.* Edited by William J. Hall. Vol. 4th Edition. Berkeley, San Francisco, California: Pearson Education, Inc. publishing as Prentice Hall, 2012.

Clara, Tiago Barosa. *Added Mass Effects on the Natural Frequencies of Marine Current Turbine Blades.* Master Thesis, Fachgebiet Strömungsmaschinen, Karlsruhe: Karlsruhe Institute of Technology, 2014.

Clara, Tiago, J.A.C. Falcão de Campos, and J. Baltazar. *Added Mass Effects on the natural frequencies of marine current turbine blades.* Extended Abstract of Master Thesis, Ponta Delgada/Azores: MARETEC, 2015.

Clough, Ray W., and Joseph Penzien. *Dynamics of Structures - International Student Edition.* Tokyo: McGraw-Hill International Book Company, 1975.

Conca, James. *Tidal Energy - - All Renewables Are Not Created Equal - Forbes.* 27th June 2017. https://www.forbes.com/sites/jamesconca/2017/07/27/tidal-energy-all-renewables-are-not-created-equal/#588525c94f4e (accessed June 12th, 2018).

Faria, Luis. "Discussion about the Master Thesis." June 2018.

Fish, Jacob, and Ted Belytschko. *A First Course in Finite Elements.* Chichester, West Sussex: John Wiley & Sons Ltd., 2007.

Frewin, Chris. *Renewable Energy - STUDENTENERGY.* 17th May 2015. https://www.studentenergy.org/topics/renewable-energy (accessed August 30th, 2018).

GEOGRAPHIC, NATIONAL. *Tidal Energy - National Geographic.* 2018. https://www.nationalgeographic.org/encyclopedia/tidal-energy/ (accessed August 31st, 2018).

Götz, Sören. "ZEIT ONLINE." 5th September 2017. http://www.zeit.de/wirtschaft/2017-08/co2-steuer-klimawandel-abgas-skandal/komplettansicht (accessed January 4th, 2018).

Hanania, Jordan, Kailyn Stenhouse, and Jason Donev. *Energy Education - University of Calgary.* 29th August 2017. https://energyeducation.ca/encyclopedia/Energy_from_ocean_waves (accessed August 31st, 2018).

IEA. "Renewables - International Energy Agency." *International Energy Agency.* 4th October 2017. https://www.iea.org/topics/renewables/ (accessed August 30th , 2018).

Kanniah, Geetha. *Fossil Fuels - STUDENTENERGY.* 17th May 2015. https://www.studentenergy.org/topics/fossil-fuels (accessed August 30th , 2018).

McBain, J. C., R. E. Kielb, and A. W. Leissa. "Vibrations of Twisted Cantilevered Plates - Experimental Investigations." *29th International Gas Turbine Conference and Exhibit.* Amsterdam: American Society of Mechanical Engineers, 1984. Paper Number 84-GT-96.

Philibert, Cédric. *Renewable Energy for Industry - From green energy to green materials and fuels.* IEA - Insight Series 2017, Paris: International Energy Agency, 2017.

Ramos, Helena. *Guideline for Design of SMALL HYDROPOWER PLANTS.* Belfast: Western Regional Energy Agency & Network and Department of Economic Development, 2000.

Rossi, Mosè, Maurizio Righetti, and Massimiliano Renzi. "Pump-as-Turbines for energy recovery applications: the case study of an aqueduct." *71st Conference of the Italian Thermal Machines Engineering Association.* Turin: Libera Università di Bolzano, 2016.

Sarmento, António, Falcão José Alberto De Campos, Luís Eça, Luís Miguel Chagas Costa Gil, Eric Didier , and João Baltazar. *Marine Technology - Homepage.* 2009. http://maretec.tecnico.ulisboa.pt/marine_technology.htm (accessed August 27th, 2018).

Sigrist, Jean-François. *Fluid-Structure Interaction, An Introduction to Finite Element Coupling.* Chichester, West Sussex: John Wiley & Sons Limited, 2015.

Simulia. *26.1.1 Element library: overview.* July 5th 2011. http://ivt-abaqusdoc.ivt.ntnu.no:2080/v6.11/books/usb/default.htm?startat=pt06ch27s01alm01.html (accessed April 25th , 2018).

Soares, Carlos Guedes. *Research & Development.* 2006. http://www.centec.tecnico.ulisboa.pt/en/centec/index.aspx (accessed August 27th, 2018).

Staud, Toralf. *Zeitleiste: Die Internationalen Klimaverhandlungen, eine Chronik - Bundeszentrale für politische Bildung.* 10th February 2015. http://www.bpb.de/gesellschaft/umwelt/klimawandel/200832/zeitleiste-die-internationalen-klimaverhandlungen-eine-chronik (accessed August 29th, 2018).

Stephan, Pascal. *Suitable Bonding Method of a Multi-Material Glove Compartment for Lightweight Design.* Bachelor Thesis, School of Engineering Science, Engineering and Technology, Skövde: Högskolan i Skövde, 2016, 3-4.

UN. "The Paris Agreement." *United Nations Climate Change.* 3rd July 2018. https://unfccc.int/process-and-meetings/the-paris-agreement/the-paris-agreement (accessed August 29th, 2018).

US-EIA. *Hydropower Explained - Tidal Power.* 28th August 2018. https://www.eia.gov/energyexplained/index.php?page=hydropower_tidal (accessed August 31st, 2018).

von Wirth, Timo, Linda Gislason, and Roman Seidl. "Journals & Books - Science Direct." *ScienceDirect.* 15th October 2017. https://www.sciencedirect.com/science/article/pii/S1364032117313412 (accessed August 30th, 2018).

Wall, Alex. *Top 10 Nuclear Disasters.* 2012. http://www.processindustryforum.com/hottopics/nucleardisasters (accessed August 30th, 2018).

Young, Yin L., Michael R. Motley, and Ronald W. Yeung. "Three-Dimensional Numerical Modelling of the Transient Fluid-Structure Interaction Response of Tidal Turbines." Edited by Takeshi Kinoshita. *Journal of Offshore Mechanics and Arctic Engineering*, 2010: Vol. 132 / 011101-1.

Young, Yin Lu Julie. "Time-dependent hydroelastic analysis of cavitating propulsors." *Journal of Fluids and Structures*, November 2006: 269-295.

Appendix

Appendix Table 1: Relative error between results for the natural frequencies of the MCT blade in water and in air compared to Young (Y) and Tiago Clara (TC), mistakes are in percentages, mesh and elements are describing the mesh and elements used in this work

Description	EL	Mesh	Mode 1	Mode 2	Mode 3
Error Y vs TC Air			-24.54	-7.93	-1.28
Error Y vs TC Water			-40.00	-24.37	-9.64
Error FEM I vs Y AIR	C3D8R, C3D6	1 EL over thickness	54.05	55.93	37.28
Error FEM I vs Y AIR	C3D20, C3D15	1 EL over thickness	-33.37	-9.14	-1.26
Error FEM I vs Y WATER	C3D8R, C3D6, AC3D4	1 EL over thickness	43.61	43.90	45.03
Error FEM I vs Y WATER	C3D20, C3D15, AC3D10	1 EL over thickness	-58.21	-28.73	-9.31
Error FEM II vs Y AIR	C3D8R, C3D6	3 EL over thickness	-29.38	-8.25	1.98
Error FEM II vs Y AIR	C3D20, C3D15	3 EL over thickness	-33.20	-9.00	-1.25
Error FEM II vs Y WATER	C3D8R, C3D6, AC3D4	3 EL over thickness	-61.08	-29.40	-4.50
Error FEM II vs Y WATER	C3D20, C3D15, AC3D10	3 EL over thickness	-57.67	-28.00	-7.56
ERROR FEM I vs TC AIR	C3D8R, C3D6	1 EL over thickness	65.32	59.43	38.08
ERROR FEM I vs TC AIR	C3D20, C3D15	1 EL over thickness	-0.64	-0.49	0.03
ERROR FEM I vs TC WATER	C3D8R, C3D6, AC3D4	1 EL over thickness	66.17	57.57	50.32
ERROR FEM I vs TC WATER	C3D20, C3D15, AC3D10	1 EL over thickness	5.07	2.64	1.23
ERROR FEM II vs TC AIR	C3D8R, C3D6	3 EL over thickness	2.37	0.33	3.23
ERROR FEM II vs TC AIR	C3D20, C3D15	3 EL over thickness	-0.52	-0.36	0.04
ERROR FEM II vs TC WATER	C3D8R, C3D6, AC3D4	3 EL over thickness	3.35	2.13	5.57
ERROR FEM II vs TC WATER	C3D20, C3D15, AC3D10	3 EL over thickness	5.40	3.19	2.81
ERROR FEM IV vs TC AIR	C3D8R, C3D6	20 EL over thickness	-1.59	-1.99	1.91
ERROR FEM IV vs TC AIR	C3D20, C3D15	20 EL over thickness	-0.57	-0.37	0.21
ERROR FEM IV vs TC WATER	C3D8R, C3D6, AC3D4	20 EL over thickness	2.48	-0.78	2.72
ERROR FEM IV vs TC WATER	C3D20, C3D15, AC3D10	20 EL over thickness	5.43	3.24	2.95